Electronic Supplementary Material (ESI) for ChemComm.

Electronic Supporting Information for

A new concept of transparent photocapacitor

Elena Navarrete-Astorga[a], Daniel Solís-Cortés[a], Jorge Rodríguez-Moreno[a], Enrique A. Dalchiele[b], Ricardo Schrebler[c], Francisco Martín[a] and José R. Ramos-Barrado[a].

a Universidad de Málaga. Andalucía Tech. Departamentos de Física Aplicada & Ingeniería Química. Laboratorio de Materiales y Superficies (Unidad Asociada al CSIC), E29071 Málaga, Spain.

b Instituto de Física, Facultad de Ingeniería, Herrera y Reissig 565, C.C. 30, 11000 Montevideo, Uruguay.

c Instituto de Química, Facultad de Ciencias, Pontificia Universidad Católica de Valparaíso, Casilla 4059, Valparaíso, Chile

1. Preparation of the samples

The transparent device was composed by a TiO_2 photoanode, a $LiFeO_2$-Ag counter electrode and an electrolyte.

The TiO_2 photoanode films have been deposited by DC magnetron sputtering on ITO/glass substrates after being previously sequentially ultrasonically cleaned in acetone, isopropanol and finally distilled water, 5 minutes in each solvent. A titanium target (99.9%) from *AJA International, Inc.* was employed. The power was set at 300 W. The working pressure into the vacuum chamber remained constant at 3 mTorr with a high purity (5.0) Ar gas and O_2 gas, each regulated by mass flow controllers at 18 sccm and 3.23 sccm, respectively. The equipment used was a Magnetron Sputtering System ORION-5-UHV (*AJA International, Inc.*).

The $LiFeO_2$-Ag thin film electrode was obtained by spray pyrolysis, heating at 450 ºC during 1 hour, and using a precursor solution described in a previous work by our group[1]. There were tested two types of electrolyte in our photocapacitor. The first one was an electrolyte based on PVP/$LiClO_4$ developed by us[2] and the second one an ion gel electrolyte composed by PVP/[HEMIm][BF_4], which preparation and characterization was detailed in our previous work as well[3].

Finally, the photocapacitor was assembled with the three components described previously.

2. Characterization and electrochemical techniques

Laboratory X-ray diffraction (XRD) patterns were collected on a PANanalytical X'Pert Pro automated diffractometer. Patterns were recorded in Bragg-Brentano reflection configuration by using a Ge(111) primary monochromator (Cu Kα 1) and the X'Celerator detector with a step size of 0.017º (2θ). The patterns were recorded between 10 and 80 degress in 2θ with an overall measuring time of 32 minutes.

X-Ray photoelectron spectra were recorded on a Physical Electronics PHI 5700 spectrometer, using non-monochromated Mg Ha radiation.

Field-emission scanning electron microscopy (FE-SEM) pictures of the electrodes were obtained on a Helios Nanolab 650 Dual Beam from FEI company equipment.

An atomic force microscope (AFM) was used to examine the surface morphology of the electrodes. Topographics AFM examinations were performed by using a Nanoscope V tapping-mode AFM (Veeco Instruments) employing sharp silicon tips.

The electrochemical performance of the resulting supercapacitor was evaluated by cyclic voltammetry (CV), galvanostatic charge-discharge (GCD) and electrochemical impedance spectroscopy (EIS) processes carried out with a Biologic Potentiostat VSP. Photo-charge/galvanostatic-discharge measurements were carried out by Autolab PGSTAT30 potentiostat under illumination (100 mW cm^{-2}) of simulated AM1.5G solar light coming from a solar simulator (Oriel Xe lamp of 500 W). To measure the variation of the potential with the irradiation (photo-charge), the TiO_2 electrode was used as the working electrode and the $LiFeO_2$ as counter-reference electrode.

For visible range (300–900 nm) transmission measurements, a Varian Cary 1E was used. The performance of the resulting photocapacitor was evaluated by cyclic voltammetry and photo-charge/self-discharge processes carried out with an Autolab PGSTAT30 potentiostat. To measure the variation of the potential with the irradiation (photo-charge), the TiO_2 electrode was used as the working electrode and the $LiFeO_2$ as counter-reference electrode. A Hg lamp was used to irradiate the TiO_2 electrode in an hour recess of dark-irradiation to measure the potential between both electrodes.

3. Morphological characterization of the electrodes by FE-SEM

The thickness of the $LiFeO_2$ and the TiO_2 electrodes was directly obtained by FESEM pictures. Fig. S1 shows the morphology of the films and the cross-sections carried out to measure the thickness, which was ca. 130 nm for the $LiFeO_2$ and ca. 790 nm for the TiO_2.

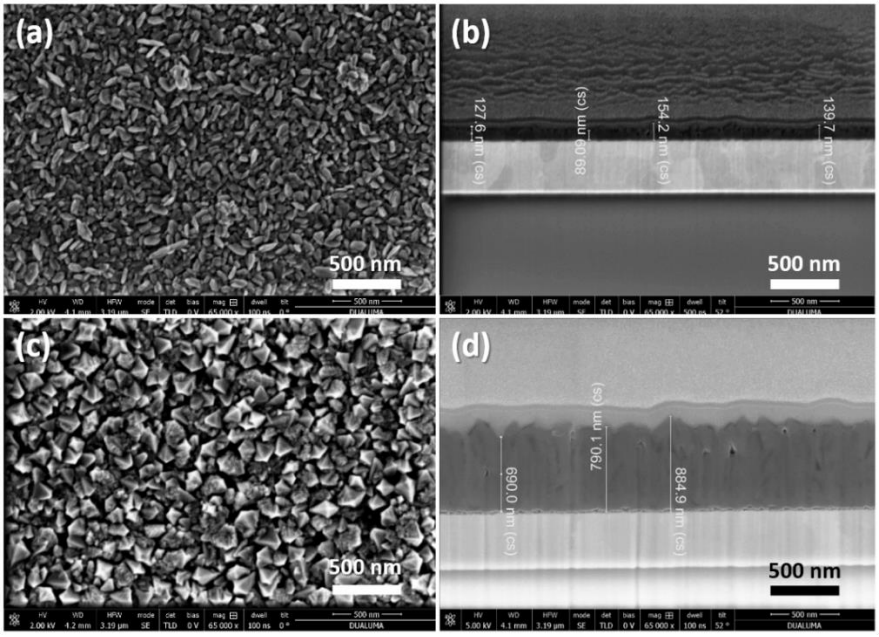

Fig. S1. FE-SEM top view pictures (a, c) and cross-sections (b, d) of $LiFeO_2$ (a,b) and TiO_2 (c,d) thin films deposited on the ITO substrate.

4. Characterization of the photo-electrode of TiO_2

From the result of XRD measurement (Fig. S2), it was observed that the TiO_2 prepared by DC reactive sputter deposition at 623 K had rutile structure with the crystallite size of ca. 32 nm from Scherrer equation, without reflections of anatase or brookite.

XPS study was carried out to confirm the stoichiometry of TiO_2 films. In samples prepared at 200W, the XPS Ti $2p_{3/2}$ and $2p_{1/2}$ peaks of TiO_2 were shown at ca. 459.48 and 459.01 eV respectively. On the other hand, samples prepared at 300W showed more reduced, showing the XPS Ti $2p_{3/2}$ and $2p_{1/2}$ peaks of TiO_2 at ca. 459.43 and 459.04 eV.

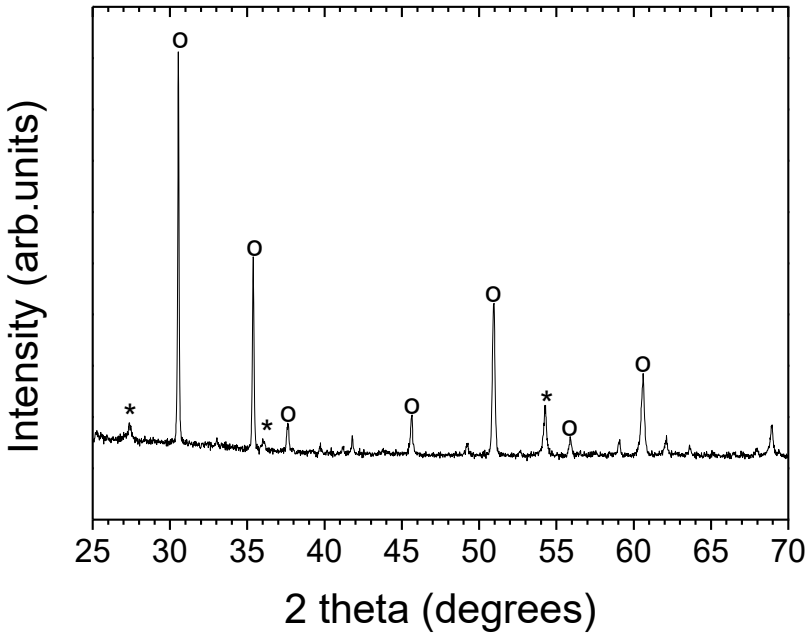

Fig. S2. XRD pattern for the TiO_2 thin film deposited on the ITO substrate. It is shown rutile peaks (*) and ITO peaks (○).

5. AFM

The roughness of the $LiFeO_2$ and the TiO_2 electrodes was measured through AFM, being 14.3 nm and 31.3 nm respectively. Fig. S3 shows the AFM pictures for both electrodes, taking an area of 1 μm^2.

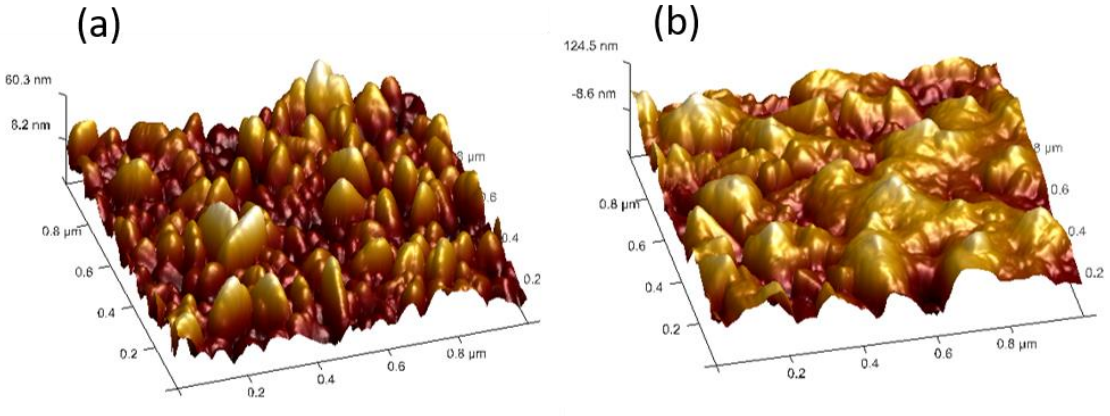

Fig. S3. AFM for $LiFeO_2$ (a) and TiO_2 (b) thin films deposited on the ITO substrate.

6. Optical measurements

Transmittance results for all the separated components of the photocapacitor and the photocapacitor itself are shown in Fig. S4. At λ= 555 nm (optical transmittance evaluated at this wavelength because the photopic eye sensitivity function has maximum sensitivity in the green spectral range at 555 nm), the transmittance of the different components of the photocapacitor was the following: 77% for the TiO_2 electrode, 67% for the $LiFeO_2$-Ag electrode and 91% for the ion gel electrolyte, being the transmittance at 555 nm for the whole device 57%.

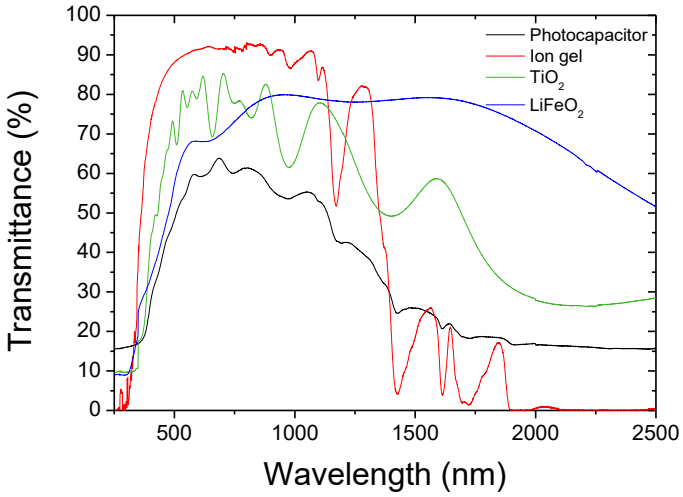

Fig. S4. Optical transmittance of each electrode, the ion gel electrolyte and the photocapacitor itself.

7. Overall efficiency ($\eta_{overall}$) of the photocapacitor

The $\eta_{overall}$ of the photocapacitor was calculated according the equation eq. S1[4], where E_{sp} is the specific energy, E_{light} the incident light power density (100 mW cm^{-2}) multiplied by the photocharge time and $A_{photocap.}$ the area of the photocapacitor (6 cm^2).

$$\eta_{overall} = \frac{E_{sp}}{E_{light} \cdot A_{photocap.}} \qquad (eq.S1)$$

References

1 F. Martín, E. Navarrete, J. Morales, C. Roldán, J. R. Ramos-Barrado and L. Sanchez, *J. Mater. Chem.*, 2010, **20**, 2847–2852.

2 J. Rodríguez-Moreno, E. Navarrete-Astorga, E. A. Dalchiele, L. Sánchez, J. R. Ramos-Barrado and F. Martín, *J. Power Sources*, 2013, **237**, 270–276.

3 E. Navarrete-Astorga, J. Rodríguez-Moreno, E. A. Dalchiele, R. Schrebler, P. Leyton, J. R. Ramos-Barrado and F. Martín, *J. Solid State Electrochem.*, 2017, **21**, 1431–1444.

4 Y. Jin, Z. Li, L. Qin, X. Liu, L. Mao, Y. Wang, F. Qin, Y. Liu, Y. Zhou and F. Zhang, *Adv. Mater. Interfaces*, 2017, **4**, 1700704.